Electronic structure of pyrite-type manganese disulphide (pMnS$_2$): An *ab initio* study

Rémy Tappero, Isabelle Baraille, and Albert Lichanot

Laboratoire de Chimie Structurale, UMR 5624, Université de Pau et des Pays de l'Adour, IFR, rue Jules Ferry, 64000 Pau, France

The linear combination of atomic orbitals as implemented in the CRYSTAL95 code has been used to obtain the electronic structure of the pyrite-type manganese disulphide in the ferromagnetic state. Calculations made at the unrestricted Hartree-Fock (UHF) and local density approximation levels show that this compound has a larger ionic character within the HF approach. The band structures obtained with both methods of calculation are significantly different. In particular, the valence band is mainly occupied by the p orbitals of sulfur in the UHF approach and the compound is described as an insulator, whereas, at the LDA level, the Mn d orbitals also lie in this band and the compound then has a conductor character. [S0163-1829(98)02227-9]

INTRODUCTION

Pyrite-type structures of transition-metal dichalcogenides have undergone intensive investigations in recent years due to their varied electrical and magnetic properties. Magnetic structure[1,2] and ordering,[3,4] antiferromagnetic phase transition[5–7] and spin correlations[8] of the manganese disulphide have drawn particular attention in stating precisely its magnetic properties. These studies (in particular by neutron diffraction) show that the pyrite-type phase of MnS$_2$ (pMnS$_2$) has an antiferromagnetic ordering of the third kind (AF$_3$) below 48 K involving a doubling of the chemical cell in the direction where the moments alternate.[1,6] They confirm as does the magnetic susceptibility, that Mn has the high-spin d^5 configuration, thus eliminating the possibility of a significant degree of π backbonding between manganese and sulfur.[9] The magnetic moment per Mn has been found to be about $5\mu_B$ (Ref. 7) suggesting that pMnS$_2$ could be regarded as an essentially ionic compound. High pressure x-ray diffraction[10,11] also shows that pMnS$_2$ is rather compressible with a bulk modulus of 76 GPa, and that a pressure effect induces at about 14 GPa a structure transition from the pyrite to the marcasite-type phase accompanied by a large volume contraction (15%). Mössbauer resonance studies[12] suggest that this transition is of high-spin–low-spin type. In contrast to the magnetic structure, the electronic structure of pMnS$_2$ has not been investigated in any depth. To our knowledge, no detailed band structure and charge density calculations have so far been reported. Only one study[13] reports the density of states of pMnS$_2$ calculated from the linear muffin tin orbital atomic sphere approximation method for 10 eV above and below the Fermi level. However, neither the shape of the band structure associated with this density of states nor the separation between the behavior of the spin up and spin down electrons is given. From this study, pMnS$_2$ is found in a metallic ground state characterized by the location of the manganese d bands above the sulfur p ones. In two other papers, general information is also available: (i) tentative bonding schemes deduced from hypothetical energy band diagrams and leading to a band gap close to 1 eV are given by Brostigen and Kjekshus[14] and (ii) the gross features of the energy level scheme could be rationalized by Goodenough[15] from symmetry arguments of the pyrite structure.

In this work, the linear combination of atomic orbitals (LCAO) self-consistent-field (SCF) method implemented in the CRYSTAL95 code[16] is used to calculate the electronic structure and spin density of pMnS$_2$ in the ferromagnetic state. The study of this state is justified because it is considered as a reference when determining the exchange energy pairs, J, involved in a model (Heisenberg or Ising) spin Hamiltonian of the antiferromagnetic solution. Given the small J values reported (in the literature[3,7,17]), the energy difference between the ferromagnetic and antiferromagnetic solutions is small, as in the more simple systems MnO, NiO,[18] and MnS.[19] Properties depending on total energy such as charge and spin densities and band structures are thus very similar for the two solutions. The calculations have been made at two levels of approximation using (i) the unrestricted Hartree-Fock (UHF) approach and (ii) the density functional theory (DFT) method where the exchange and correlation potentials are parametrized according to the local density approximation (LDA) models of Dirac[20] and Perdew-Zunger,[21] respectively. As in the HF approximation, the DFT wave function is obtained by solving self-consistently the Kohn-Sham (KS) one electron equations.

The aim of this paper is to obtain the electronic structure of pMnS$_2$ in its ferromagnetic state. For that, the Mulliken population corresponding to the charge and spin distributions, the band structure and associated density of states, and the charge and spin densities are calculated both at the UHF and DFT-LDA levels. Comparison of the two sets of calculations allows us to evaluate the contribution of a part of the electron correlation taken into account in the LDA approach. Physical parameters such as lattice parameter and sulfur fractional position in the cell, binding energy, and bulk modulus are before performed and compared to experiment in order to test the adequacy of the computational parameters and orbital atomic basis set used in this study.

I. STRUCTURE OF THE PYRITE-TYPE MANGANESE DISULPHIDE AND COMPUTATIONAL PROCEDURE

The pyrite-type structure is primitive cubic [space group $P_{a\bar{3}}(T_h^6)$, $Z=4$]. It is characterized by a NaCl-like arrangement of manganese atoms and disulphide groups (S$_2$). The centers of three S$_2$ groups are located in the middle of the cube edges and the fourth group at the center of the cell; their

axis points along the four-body diagonals. At 298 K, the lattice parameter is 6.104 Å and the atomic positions are Mn(0,0,0) and S(0.4011, 0.4011, 0.4011).[22] For this geometry, the interatomic distances and angles are: Mn-S $= 2.593$ Å, S-S $= 2.091$ Å, $\widehat{MnSMn} = 112.7°$, and $\widehat{SSMn}$ $= 106.0°$. The manganese atoms are sixfold coordinated by distorted octaedra of S atoms whereas each S atom is tetrahedrally (distorted) bonded to three Mn and one S atoms. For clarity, only the (011) plane of this structure is given in Fig. 5.

The crystalline wave-function calculation was performed using the CRYSTAL95 code.[16] An exhaustive description of the periodic Hartree-Fock crystalline orbital SCF computational scheme embodied in this code is already available.[23] As regards the computational conditions, the numerical values of the tolerance parameters involved in the evaluation of the infinite bielectronic Coulomb and exchange series are the standard values[23] and are chosen to ensure high numerical accuracy. The shrinking factor, defining the reciprocal space net corresponds to 11 reciprocal space points in which the Fock matrix is diagonalized. In the CRYSTAL95 code, an unrestricted Hartree-Fock option is available for the treatment of spin polarized systems and is used for pMnS$_2$ due to the presence of unpaired d electrons on Mn. In the UHF formulation, only the total number of unpaired electrons in the unit cell is imposed a $priori$ whereas no constraint is imposed on the partition of the spin density among the d orbitals of manganese. The final spin configuration in the unit cell is thus the result of a variational calculation with the constraint of an a $priori$ defined number of (α-β) electrons. In this code, the density functional theory, in the local density approximation (LDA), has recently been introduced to the self-consistent field (SCF) process, resolving at each stage the Khon-Sham (KS) equations rather than the HF equations. The exchange part of the HF monoelectronic operator is replaced by an exchange-correlation potential, which is the functional derivative of the exchange-correlation density functional energy. Details of numerical calculations are given elsewhere.[24]

The all-electron atomic orbitals (AO) basis set adopted to describe Mn (8-6411G**) and S (8-6311G) atoms within the unit cell have already been described in the study of MnO (Ref. 18) and Li$_2$S (Ref. 25), respectively. The exponents of the most diffuse sp shells of each atom and the d shell of manganese have been optimized by searching for the minimum crystalline total energy corresponding to the experimental volume.

II. RESULTS

A. Equilibrium geometry and energy

The calculated equilibrium structural configuration has been obtained by minimizing the total energy with respect to the lattice parameter "a" and the sulfur fractional coordinate x(S). Steps of 0.05 Å and 0.002 were considered for the two variables, respectively. At first, the cell edge was only changed keeping x(S) fixed at the experimental value; x(S) was then changed separately. The data reported in Table I result from the best fit with respect to the Murnaghan equation of state[26] for 13 volumes around the experimental one.

TABLE I. Geometry [lattice parameter a (Å), sulfur fractional position x(S), Mn-S, S-S distances (Å), and $\widehat{MnSMn}$, $\widehat{SSMn}$ angles (deg)], binding energy BE (a.u.) and bulk modulus B_0 (GPa) of pMnS$_2$ calculated at the HF and LDA levels.

	HF	LDA	Expt.
a	6.448	6.129	6.083[a]
x(S)	0.4007	0.3913	0.4008[a]
Mn-S	2.739	2.578	2.591[a]
S-S	2.211	2.293	2.091[a]
$\widehat{MnSMn}$	112.8	114.3	112.8[a]
$\widehat{SSMn}$	105.9	104.0	105.9[a]
BE	0.21	0.29	0.39[b]
B_0	70.4	92.0	76.0[c]

[a]Reference 22.
[b]Calculated at 0 K from Janaf Tables (Ref. 30).
[c]References 10, 11.

The experimental values determined at 15 K by neutron diffraction[22] are also given in Table I. They can be considered as good values to be compared to our results calculated at the 0 K temperature. Table I confirms the well-known tendency of HF calculations to overestimate the lattice parameters. In this case, the overestimation (6%) is similar to that observed in MnS (4.5%) (Ref. 19) but is greater than that obtained with oxides such as MnO (1.8%).[18] It is attributable to sulfur belonging to a higher row of the periodic table. The part of the electron correlation introduced in the LDA approach greatly improves the "a" value. However, the S fractional position x(S) is deteriorated with respect to the experiment. As a result, the HF approach increases the Mn-S and S-S distances whereas the LDA approach increases the S-S bond (9.5%) in particular without modifying the Mn-S one. It has to be noted that in both cases the S-S distance remains very close to that calculated for the isolated S$_2^{2-}$ molecular anion [2.020 Å (Ref. 27)]. The values of the $\widehat{MnSMn}$ and $\widehat{SSMn}$ angles that depend only on the x(S) value are slightly increased and decreased, respectively. The binding energy (BE) has been calculated with respect to the neutral atoms in their ground states. The Mn and S atoms are described with the same basis set as for the bulk supplemented by two sp and one d functions and the three most diffuse shells are reoptimized. As expected, the BE is underestimated by 45% when calculated at the HF level. This result is greater than that obtained for closed-shell oxides.[28] The LDA approach improves this result significantly, which is not surprising given that the HF approach neglects the electron correlation. Finally the bulk modulus B_0, which is well reproduced at the HF level, is greatly increased in the LDA calculations as a consequence of a more compact geometry obtained in this approach.

B. Electronic structure and spin density

All the electronic properties have been determined for the experimental geometry to compare the HF and the LDA calculations validly with the experimental data. First, we consider the Mulliken population analysis reported in Table II. The HF net charges on the Mn and S$_2$ group are $\pm 1.76|e|$,

TABLE II. Mulliken population data in $|e|$. Total charge ($\alpha + \beta$) and net spin ($\alpha - \beta$) in the valence atomic orbitals and bond populations are calculated at the HF and LDA (in parentheses) levels for the experimental geometry.

	Mn $(\alpha+\beta)$	Mn $(\alpha-\beta)$	S $(\alpha+\beta)$	S $(\alpha-\beta)$
sp	7.98 (8.01)	0.02 (0.03)	6.90 (6.73)	0.05 (0.10)
$d(t_{2g})$	3.07 (3.27)	2.96 (2.63)		
$d(e_g)$	2.11 (2.25)	1.93 (1.65)		
total d	5.18 (5.52)	4.89 (4.28)		
net charge	+1.76 (+1.38)	+4.90 (+4.31)	−0.88 (−0.69)	+0.05 (+0.10)
Mn-S	0.00 (0.01)	−0.02 (−0.04)		
S-S	−0.47 (−0.52)	−0.04 (−0.02)		

while the corresponding LDA ones are $\pm 1.38|e|$. By considering the ideal ionic state as a reference (Mn^{2+}, S_2^{2-}), the charge transfer from the molecular anion towards manganese is three times higher in the LDA calculations than in the HF approach, which reports a situation close to the ideal ionic one. This last result is supported by the d population analysis, which leads to an electronic high spin configuration $t_{2g}^3 e_g^2$ (Mn) characterizing Mn^{2+} in an octahedral environment. The calculated magnetic moment per Mn^{2+} ($4.90\mu_B$) describes the $^6S_{5/2}$ ground state well and agrees well with the effective moment measured [$6.16\mu_B$ (Ref. 7), $6.30\mu_B$ (Refs. 1 and 3)] from magnetic susceptibility experiments and with the exact value ($5.92\mu_B$ with $L=0$ and $S=5/2$). At the LDA level, a large part of the 0.6 electron transferred to Mn can be found in the d shell where the e_g and t_{2g} β (spin-down) states are populated by $0.30|e|$ and $0.32|e|$, respectively. This result, contributing to a decrease in the Mn^{2+} magnetic moment to $4.31\mu_B$, can be compared with previous LSD calculations on the zinc blende-type MnS,[29] which is also described as a fully ionic compound. It is associated with the mixing of unoccupied Mn d β states and an occupied S p valence band

by a p-d hybridization. The high ionic character of pMnS$_2$ is also shown by the lack of bond population between Mn and its six S nearest neighbors (Table II). However, the antibonding character between the two S atoms in the S$_2$ group that is stabilized by the crystal field effect is found to be greater in the LDA approach than in the HF approach and must be related to the large increase in the S-S distance calculated in LDA. All these results converge to confirm that the character of pMnS$_2$ is appreciably less ionic when calculated at the LDA level than at the HF one.

1. Band structures and density of states

The HF band structures associated with the α and β states of the ferromagnetic solution are shown in Fig. 1. The energy of the bottom of each band and the corresponding bandwidth are given in Table III. The two α and β narrow bands located at about −0.98 and −0.78 a.u. are pure and attributable to the $2s$ orbitals of sulfur as the projected density of states shows (Fig. 2). In the case of the α band structure, the Mn e_g and t_{2g} d states are found at −0.58 a.u. They contribute to populate the band by 37% and 60%, respectively while the remaining 3% are attributable to the $2p$ sulfur orbitals. This supports the Mulliken population analysis, which gives results very close to the ideal ionic configuration for manganese with 2.02 and 3.01 electrons in the e_g and t_{2g} orbitals, respectively. This situation is very similar to that obtained for the NaCl-type structure of MnS.[19] The $2p$ sulfur orbitals occupy almost fully the upper α and β valence bands (86% and 93%, respectively) with a small participation of the $3d$ Mn orbitals. The nearly pure valence bands and the large gaps between valence and conduction bands (9.6 and 11.2 eV for α and β states, respectively) confirm the high ionic character of pMnS$_2$. These values are largely overestimated as is generally expected in the HF approach and cannot be compared to the experimental value of about 1 eV.[14]

The band structures calculated at the LDA level (Fig. 3) exhibit conductor behavior, contrary to HF band structures. As the density of states (Fig. 4) shows, the upper valence manifold is occupied by both the manganese d orbitals and the sulfur p orbitals and presents a non-negligible (9%) mixing of Mn d β bands with sp ones. This situation leads to a substantial p-d hybridization in connection with the reduction of the calculated magnetic moment. These results are similar to those obtained by Temmerman et al.[13] performing LDA calculations in the linear muffin tin orbital atomic ap-

TABLE III. HF and LDA (in parentheses) band structures of pMnS$_2$ for the α and β electrons. The energies (in a.u.) are associated with the bottom of the bands. The corresponding bandwidths ΔE are in eV. The values are calculated for the experimental geometry at both levels.

	s(Mn)	p(Mn)	s(S)	s(S)	d(Mn)	p(S)	d(Mn)$+p$(S)
α	−3.92 (−3.04)	−2.64 (−1.95)	−0.98 (−0.72)	−0.78 (−0.55)	−0.58	−0.47	- (−0.37)
ΔE	0.0 (0.0)	0.0 (0.0)	1.1 (0.5)	1.1 (0.5)	1.1	6.8	(7.1)
β	−3.52 (−2.88)	−2.14 (−1.79)	−0.98 (−0.72)	−0.76 (−0.54)		−0.48	(−0.36)
ΔE	0.0 (0.0)	0.0 (0.0)	1.4 (0.8)	0.8 (0.5)		6.0	(6.8)
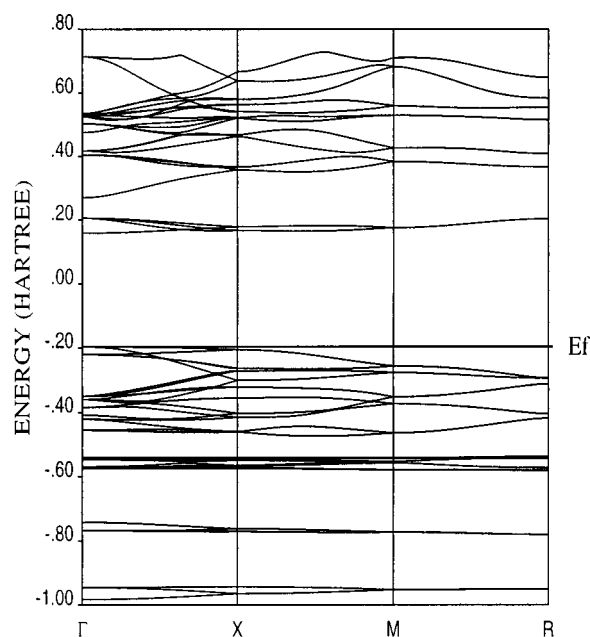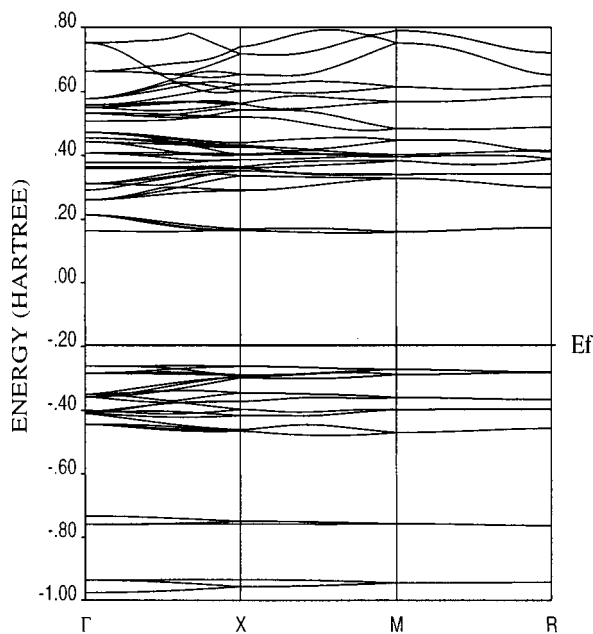
FIG. 1. HF band structures of the α (a) and β (b) states at the experimental geometry.

FIG. 2. Density of states calculated at the HF level.

proximation on low spin pMnS$_2$, but also show that allowance of a magnetic ground state does not induce a band gap as Temmerman et al. suppose. These calculations confirm that LSD approximation is able to produce the correct magnetic ground-state structure but fails to give correct band structure. This defect is attributable to the overestimation of the p-d coupling between the Mn d bands and the S p bands. According to Wei et al.,[29] this failure of LSD calculation leads to a systematic overestimation of the ordering temperature T_N, for example, on MnX^{VI} chalcogenides. Despite the
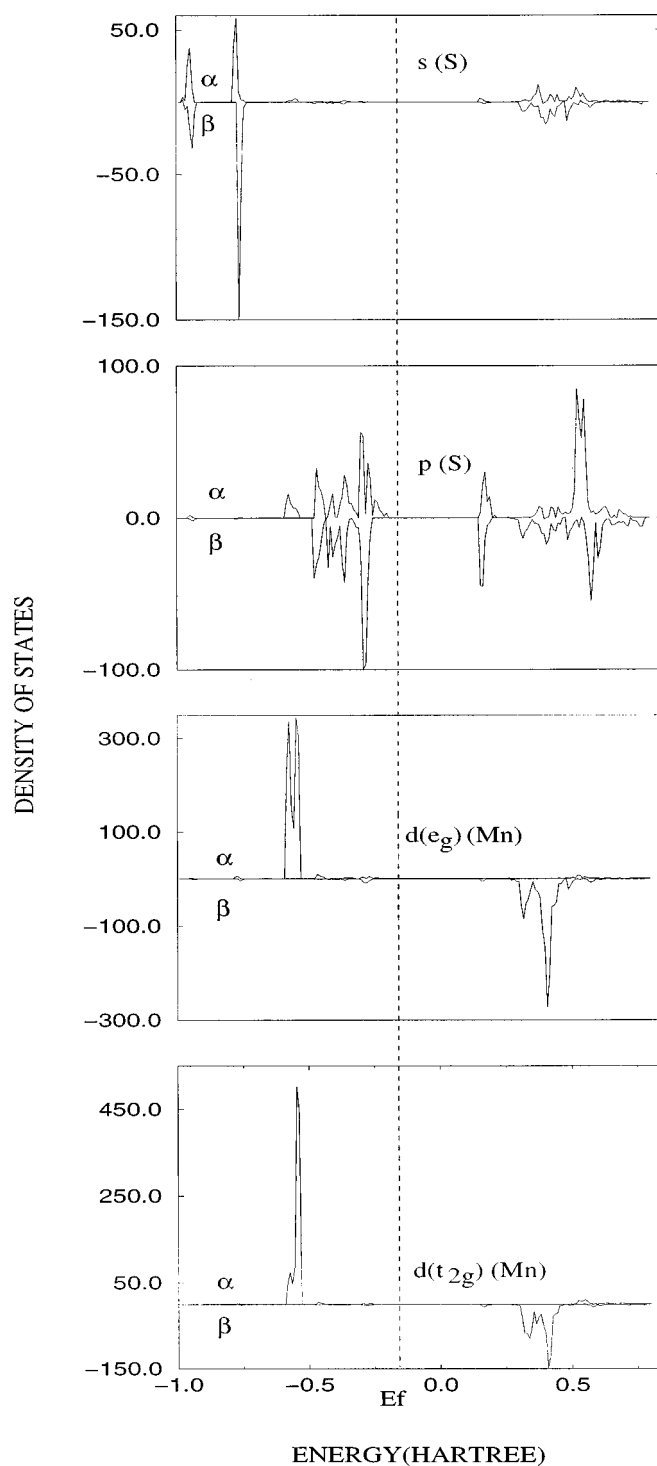
lack of correlation leading to an overestimation of the gap, HF band structures describing an ionic insulator agree with the experimental results. In contrast, LSD band structures failed to translate this character.

2. Charge and spin densities

Charge and spin densities of pMnS$_2$ have been drawn through the (011) plane of the geometrical structure (Fig. 5), which contains in particular the central molecular anion S$_2^{2-}$. Total (ECHD) and difference (DECHD) charge densi-
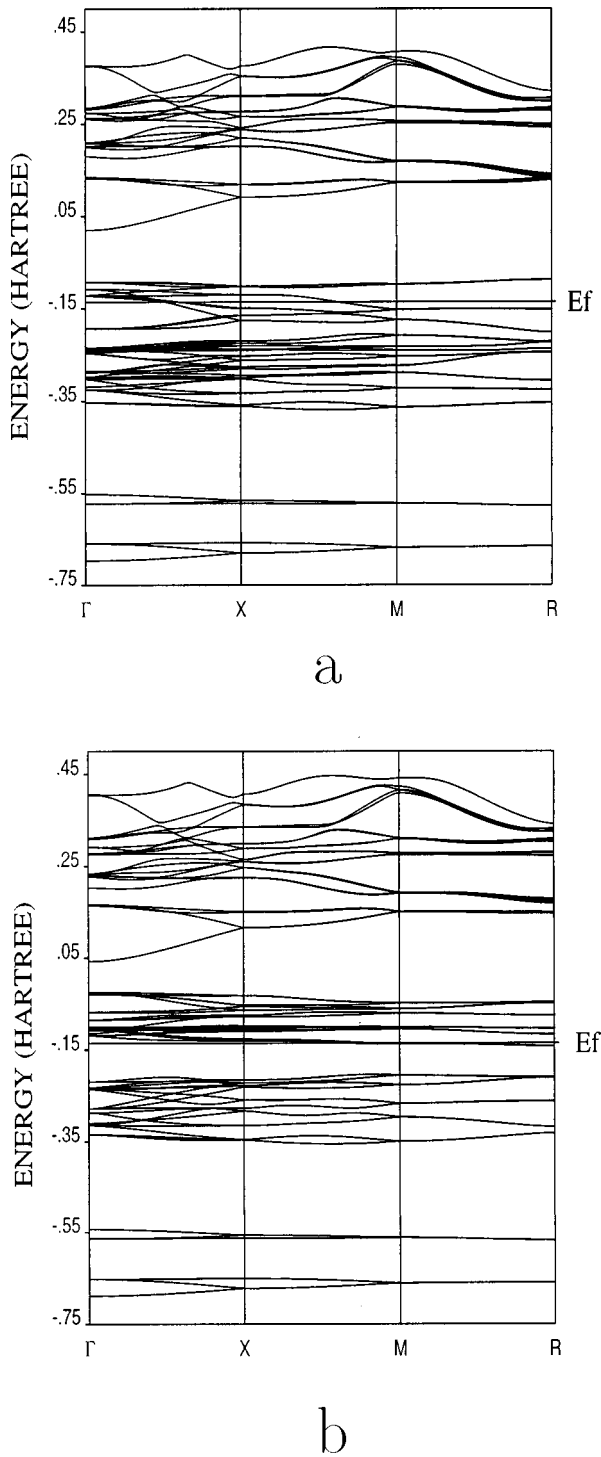
FIG. 3. LDA band structures of the α (a) and β (b) states at the experimental geometry.

FIG. 4. Density of states calculated at the LDA level.

ties are given in Figs. 6(a) and 6(b), respectively while Fig. 6(d) reports the total spin density. The DECHD map corresponds to the difference between the bulk (or total) ECHD and the charge density of the spherical free ions Mn^{2+} and S^- located on the crystal sites and described with the same basis sets as for the bulk. For reasons of clarity, only the maps calculated at the LDA level have been reported. They reproduce the same main features of the electronic structure as the HF approximation and the comparison between the two methods is illustrated by Fig. 6(c), which represents the
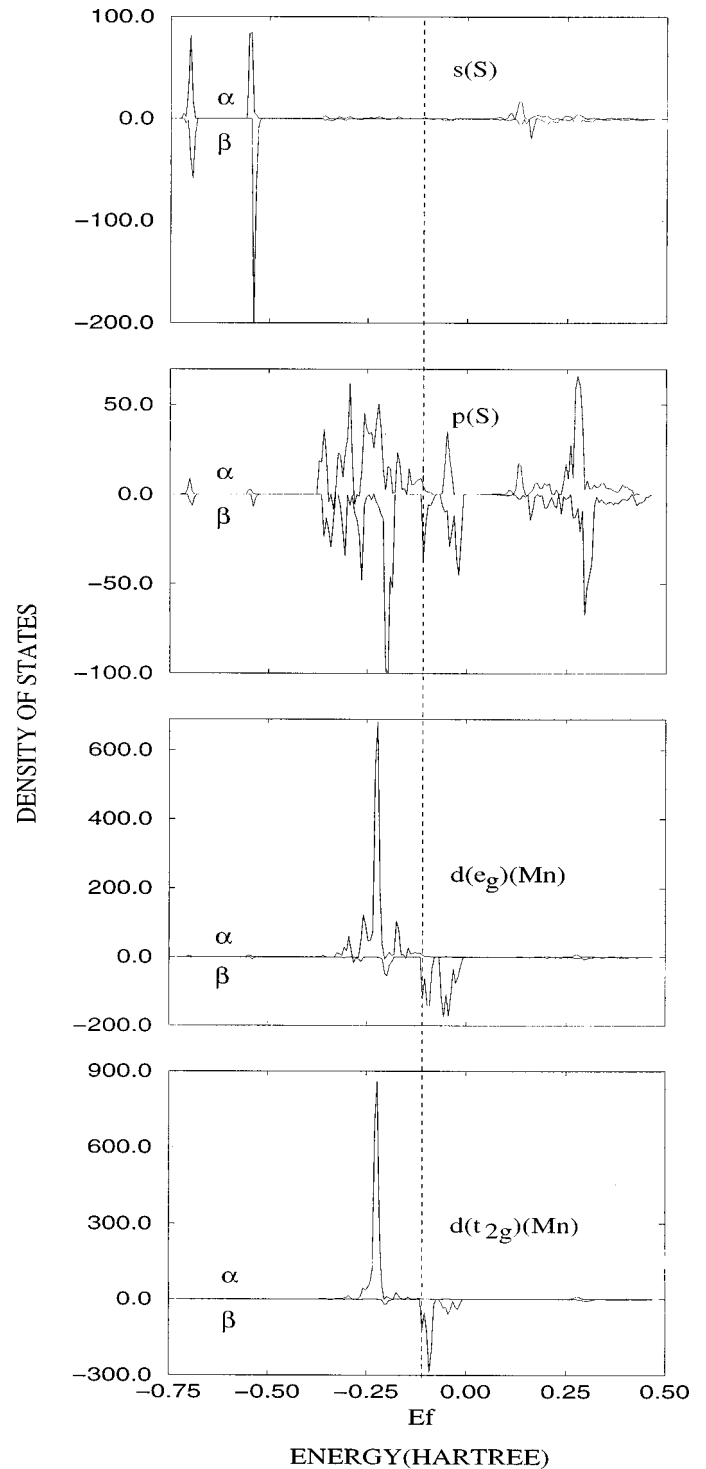
difference between HF and LDA electron charge densities. Figures. 6(a) and 6(b) show that the manganese appears as a spherical ion that is practically not deformed. However, the DECHD map [Fig. 6(b)], which gives the most accurate information about the electronic structure indicates a very small electron density (positive isodensity curves) close to Mn directed towards its nearest sulfur neighbors. The electron distribution inside and around the S_2 group is more complex and highly disturbed, particularly along two main directions. Firstly, in the Mn-S bond direction making a tetrahedral angle with the S_2 axis, the valence charge density

that corresponds both to the charge transfer from S^- (reference state) towards manganese and to the slight covalent character of the semi ionic bond, remains located near sulfur because of a greater electronegativity. This strong location compresses the electron cloud between the two sulfurs of the S_2 group to make it diffuse in the direction perpendicular to the S_2 axis. Secondly, along the [111] direction corresponding to the orientation of the S_2 group, the electron density is negative, indicating a large antibonding character between the two S atoms. This result confirms the Mulliken population analysis, which assigns a large bond population of $-0.52|e|$ to each S atom. Figure 6(c) (HF minus LDA charge densities) clearly shows a build up of charge around the S_2 group with a greater concentration along the Mn-S bond. For Mn^{2+}, a depletion of charge (dotted lines) particularly evident in the bonding direction and a build up of charge along the diagonal directions (d_{xy}, d_{xz}, and d_{yz}) are also perfectly illustrated. These results also confirm a greater ionic character of pMnS$_2$ when described in the HF approach. Finally, the map representing the total spin density [Fig. 6(d)] shows a small spin density located on the two sulfur ions, which induces a significant compression of the manganese spin density along the bond direction. It is due to sp orbitals and probably attributable through overlap terms to the Mn d orbitals.

III. SUMMARY AND CONCLUSION

The electronic structure of pMnS$_2$ in its ferromagnetic state was theoretically investigated from the LCAO-SCF method using both UHF and DFT-LDA approaches.

As regards the geometry, the two calculation methods overestimate the lattice parameter. Generally speaking, this result is well known in the HF approach and the part of the electron correlation introduced at the LDA level corrects this lattice parameter to make it smaller than the experimental one. In pMnS$_2$, the HF overestimation is too large (6%) to obtain this result. The fractional sulfur position is reproduced exactly in the HF approach, a result that must certainly be considered as fortuitous. These two parameters calculated within a given method go in opposite directions with respect to the experiment and the consequences are different: the Mn-S distance is reproduced better at the LDA level but the S-S distance is more satisfactory with the HF approach which also gives the good values of the $\widehat{MnSMn}$ and $\widehat{SSMn}$ angles. The more compact structure calculated from LDA leads to a higher value of the bulk modulus than that obtained with the HF method but agrees less with the experimental data.

Concerning the electronic structure, the HF method describes pMnS$_2$ as a practically fully ionic compound with net charges on Mn and S_2 group close to the standard ones ($\pm 2|e|$), a high spin d^5 configuration illustrated by a magnetic moment of $4.9\mu_B$, and a bond population that is zero between Mn and S. With this method, the band structure corresponds to that of an insulator. The band gap is large but, as expected, very overestimated; the bands corresponding to the different atomic orbitals are nearly pure and well separated from each other and the valence band is associated with the p orbitals of sulfur with a negligible participation of the Mn d orbitals. The electronic structure obtained from the
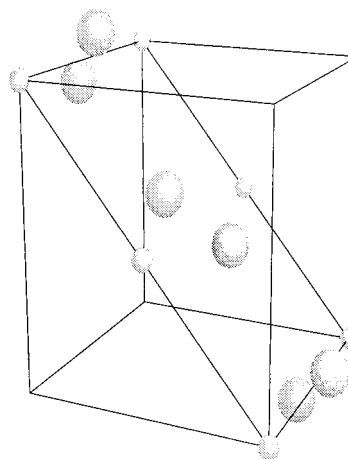
FIG. 5. Plane (011) of the pMnS$_2$ structure used as the projection plane.

LDA calculations corresponds more to a semi-ionic compound characterized by a conductor character. Indeed, the charge transfer from S_2^{2-} towards Mn^{2+} is appreciably larger than with the HF approach and remains located near the sulfur. As a consequence, the t_{2g} and e_g β states become populated by about 0.6 electron and the magnetic moment per Mn is decreased towards $4.3\mu_B$. The greatest difference between the HF and LDA calculations affects the band structure and, particularly, the valence band, and the gap value
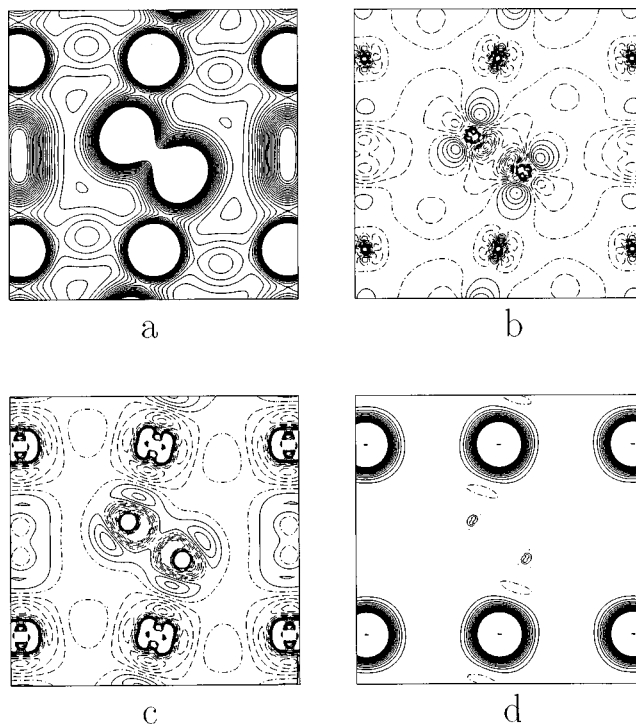
FIG. 6. Charge and spin densities projected onto the plane (011) of pMnS$_2$. (a) Total electron charge density. (b) Difference (bulk minus superposition of ionic charge distributions) electron charge density. (c) Difference (HF minus LDA) electron charge density. (d) Total spin density. Full and dashed lines correspond to positive and negative isodensity curves, respectively and the dashed-dotted line is for a zero density. The step between two consecutive isodensity curves is 0.005 a.u. except in (c) where it is 0.002 a.u.

that becomes zero in LDA. Moreover, the Mn $3d$ orbitals are destabilized and meet the manifold of the S p orbitals leading to a substantial p-d hybridization.

In conclusion, and for the specific case of pMnS$_2$ ferromagnetic state, the DFT-LDA method leads to a geometry that agrees more with experiment even if the position of sulfur in the cell and the parameters that follow are reproduced better at the HF level. As in the general case, the HF method reproduces the bulk modulus in a more satisfactory way. In contrast to the calculation of the geometry, the electronic structure of pMnS$_2$ is more comparable to the experiment when it is calculated at the HF level in spite of the very overestimated value of the band gap. In light of these conclusions, and as is widely thought, the true physics lies between the UHF and local spin density pictures. In order to examine it, two other types of calculations will be engaged in the very near future: (i) that which uses the DFT approach with an exchange-correlation potential parametrized according to the nonlocal correction of the electron density and (ii) that which mixes the HF exchange potential with the DFT correlation potential described in both the local and nonlocal approximations.

[1] J. M. Hastings, N. Elliott, and L. M. Corliss, Phys. Rev. **115**, 13 (1959).

[2] T. Chattopadhyay, P. Burlet, and P. J. Brown, J. Phys.: Condens. Matter **3**, 5555 (1991).

[3] G. van Kalkeren, R. Block, and L. Jansen, Physica B **85**, 259 (1977); **93**, 195 (1978).

[4] M. A. Saeed Khan, V. H. McCann, J. B. Ward, and R. J. Pollard, J. Phys. C **16**, 4011 (1983).

[5] J. M. Hastings and L. M. Corliss, Phys. Rev. B **14**, 1995 (1976).

[6] T. Chattopadhyay, H. G. von Schnering, and H. A. Graf, Solid State Commun. **50**, 865 (1984).

[7] M. S. Lin and H. Hacker Jr, Solid State Commun. **6**, 687 (1968).

[8] T. Chattopadhyay, Th. Brückel, and P. Burlet, Physica B **180−181**, 71 (1992); Phys. Rev. B **44**, 7394 (1991).

[9] A. Kjekshus and D. G. Nicholson, Acta Chem. Scand. **25**, 866 (1971).

[10] T. Chattopadhyay and H. G. von Schnering, J. Phys. Chem. Solids **46**, 113 (1985).

[11] T. Chattopadhyay, H. G. von Schnering, and W. A. Grosshans, Physica B **139−140**, 305 (1986).

[12] C. B. Bargeron, M. Avinor, and H. G. Drickamer, Inorg. Chem. **10**, 1338 (1971).

[13] W. M. Temmerman, P. J. Durham, and D. J. Vaughan, Phys. Chem. Miner. **20**, 248 (1993).

[14] G. Brostigen and A. Kjekshus, Acta Chem. Scand. **24**, 2993 (1970).

[15] J. B. Goodenough, J. Solid State Chem. **5**, 144 (1972).

[16] R. Dovesi, V. R. Saunders, C. Roetti, M. Causà, N. M. Harrison, R. Orlando, and E. Aprà, *CRYSTAL95 User's Manual* (University of Torino, Torino, 1996).

[17] M. S. Lin, Ph.D. thesis, University of Michigan, 1964 (unpublished).

[18] M. D. Towler, N. L. Allan, N. M. Harrison, V. R. Saunders, W. C. Mackrodt, and E. Aprà, Phys. Rev. B **50**, 5041 (1994).

[19] R. Tappero, P. D'Arco, and A. Lichanot, Chem. Phys. Lett. **273**, 83 (1997).

[20] P. A. M. Dirac, Proc. Cambridge Philos. Soc. **26**, 376 (1930).

[21] J. P. Perdew and A. Zunger, Phys. Rev. B **23**, 5048 (1981).

[22] T. Chattopadhyay, H. G. von Schnering, R. F. D. Stansfield, and G. J. McIntyre, Z. Kristallogr. **199**, 13 (1992).

[23] C. Pisani, R. Dovesi, and C. Roetti, *Hartree-Fock Ab Initio Treatment of Crystalline Systems*, Lecture Notes in Chemistry, Vol. 48 (Springer-Verlag, Berlin, 1988).

[24] M. Causà and A. Zupan, Int. J. Quantum Chem. **28**, 633 (1994).

[25] P. Azavant and A. Lichanot, Acta Crystallogr., Sect. A: Found. Crystallogr. **49**, 91 (1993).

[26] F. D. Murnaghan, Proc. Natl. Acad. Sci. USA **30**, 244 (1944).

[27] O. Knop, R. J. Boyd, and S. C. Choi, J. Am. Chem. Soc. **110**, 7299 (1988).

[28] R. Dovesi, C. Roetti, F. Freyria-Fava, E. Aprà, V. R. Saunders, and N. M. Harrison, Philos. Trans. R. Soc. London, Ser. A **341**, 203 (1992).

[29] S. H. Wei and A. Zunger, Phys. Rev. B **48**, 6111 (1993).

[30] Janaf Thermochemical Tables, 3rd ed. [J. Phys. Chem. Ref. Data **14** suppl., 1 (1985)].